THE ASTROPHYSICAL JOURNAL, 495:691–697, 1998 March 10

THE Hα LUMINOSITY FUNCTION AND STAR FORMATION RATE AT $z \sim 0.2$

LAURENCE TRESSE[1] AND STEVE J. MADDOX
Institute of Astronomy, Cambridge, CB3 0HA, England, UK
Received 1997 July 28; accepted 1997 October 14

ABSTRACT

We have measured the Hα + [N II] fluxes of the *I*-selected Canada-France Redshift Survey (CFRS) galaxies lying at a redshift z below 0.3 and hence derived the Hα luminosity function. The magnitude limits of the CFRS mean that only the galaxies with $M_B \gtrsim -21$ mag were observed at these redshifts. We obtained a total Hα luminosity density of at least $10^{39.44 \pm 0.04}$ ergs s^{-1} Mpc^{-3} at a mean $z = 0.2$ for galaxies with rest-frame EW(Hα + [N II]) $\gtrsim 10$ Å. This is twice the value found in the local universe by Gallego et al. Our Hα star formation rate, derived from Madau, is higher than the UV observations at the same z, implying a UV dust extinction of ~ 1 mag. We found a strong correlation between the Hα luminosity and the absolute magnitude in the B band: $M(B_{AB}) = 46.7 - 1.6 \log L(\text{H}\alpha)$. This work will serve as a basis of future studies of Hα luminosity distributions measured from optically selected spectroscopic surveys of the distant universe, and it will provide a better understanding of the physical processes responsible for the observed galaxy evolution.

Subject headings: galaxies: evolution — galaxies: luminosity function, mass function — galaxies: photometry

1. INTRODUCTION

Deep spectroscopic surveys recently lead to a major breakthrough in our understanding of global galaxy evolution. The Canada-France Redshift Survey (CFRS) (Lilly et al. 1995c) clearly demonstrated an evolution in the galaxy population up to a redshift $z \sim 1$, which has been confirmed by the Autofib Survey (Ellis et al. 1996). Data combining observations from the Keck Telescope and Steidel et al. (1996a) reach the star-forming galaxy population up to $z \sim 3$–4. Thus, a picture of the star formation history has emerged from these observations (Madau et al. 1996), suggesting that the peak of star formation is in the range $z = 1.3$–2.7.

The observed evolution of the galaxy population is closely related to the history of the star-forming galaxies showing spectral emission lines. Careful analysis of their spectra gives crucial information about the physical processes occurring in these galaxies (Tresse et al. 1996; Hammer et al. 1997). In the optical wavelength range, the Hα(λ6563) emission-line flux is a direct tracer of recent star formation. Massive, hot, short-lived OB stars emit ultraviolet (UV) photons, which ionize the surrounding gas to form an H II region, where the recombinations produce spectral emission lines. Of the Balmer lines, Hα is the most directly proportional to the ionizing UV stellar spectra at $\lambda < 912$ Å (see Osterbrock 1989 for a review), because the weaker Balmer lines are much more affected by the equivalent absorption lines produced in stellar atmospheres. The other commonly observed optical lines such as [N II] λλ6548, 6583, [S II] λλ6717, 6731, and [O II] λ3727, [O III] λλ4959, 5007 depend strongly on the metal fraction present in the gas. They have higher ionizing potential than the Balmer lines and thus depend also on the hardness of the ionizing stellar spectra. Therefore, they represent only indirect tracers of recent star formation.

The major factor that affects measurements of the true Hα emission fluxes is interstellar extinction. If galaxies are observed at high galactic latitudes, extinction due to our own Galaxy is negligible (~ 0.05 mag), hence most extinction is intrinsic to the observed galaxy. Star formation takes place in highly obscured regions, so extinction corrections introduce a major uncertainty in estimating the star formation rate. However, since optical wavelengths are less obscured than UV wavelengths, Hα should be a fairly good estimator of recent star formation.

One has to keep in mind that in studies where spectra are obtained for the whole galaxy, the Hα flux from OB stars is produced by H II regions that are distributed throughout both the bulge and disk. Thus, the observed line flux has been diluted by the whole stellar and interstellar content of the galaxy. Although line flux measurements depend on the content of an individual galaxy, they allow us to compare populations of galaxies at different cosmic epochs and so quantify the global physical processes of evolution. Also, if an active nucleus is present in the central region of the galaxy, then the Hα flux is not correlated directly to forming stars, but is a mixture of both. Line ratio diagrams can usually separate H II galaxies from active galaxies. However, if the active galactic nucleus (AGN) ionizing spectrum is soft, then the stellar ionizing flux can dominate, and it is more difficult to separate them. At $z < 0.3$, the number of AGN-like galaxies is roughly 10% of the number of emission-line galaxies (Tresse et al. 1996; Sarajedini et al. 1996), and so the nonstellar component is not dominant in the global Hα luminosity measurements. Nevertheless, at larger redshifts, this situation may change if there is a global evolution in the nuclear activity of galaxies.

Overall, measuring Hα fluxes in representative optically selected galaxy samples at different cosmic epochs is a major step toward the understanding of the evolutionary processes occurring within the galaxy population. The CFRS provides a preliminary sample for studies of recent star formation. Its wavelength range (4500–8500 Å) allows the measurement of Hα fluxes in galaxies at $z \leq 0.3$. A full description of the survey has been published in Lilly et al.

[1] Visiting observer with the Canada-France-Hawaii Telescope, operated by the NRC of Canada, the CNRS of France, and the University of Hawaii.

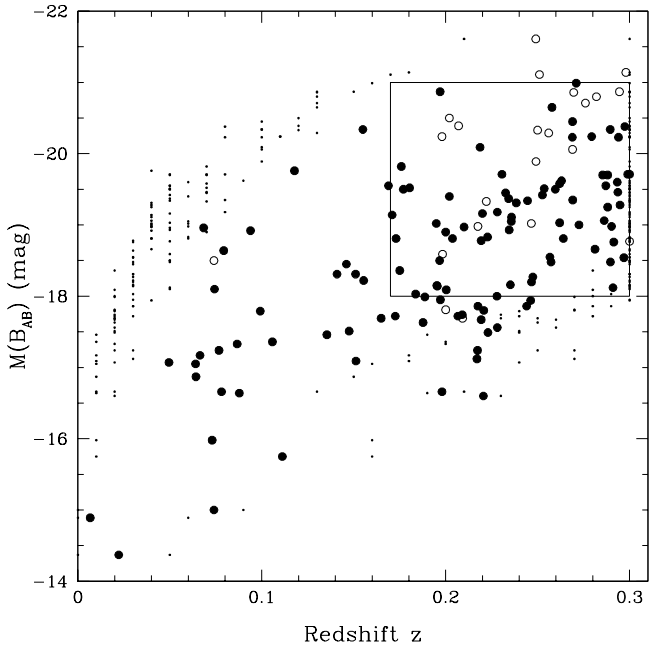

FIG. 1.—Absolute magnitudes in B_{AB} vs. redshift z of the 138 CFRS galaxies at $z \leq 0.3$. The filled circles represent Hα-emitting galaxies; the open circles show Hα-absorbing galaxies. The small dots are the minimal and maximal redshifts in which a galaxy could be detected as used in the V_{max} method (see text). The rectangle shows a homogeneous subsample of galaxies at $0.17 < z < 0.3$ and $-21 < M(B_{AB}) < -18$.

(1995a) for the photometry, in Le Fèvre et al. (1995) for the spectroscopy, in Crampton et al. (1995) for its completeness, and in particular the spectral analysis of the low-redshift sample is presented in Tresse et al. (1996, hereafter CFRS-XII).

Section 2 describes the flux measurements and the Hα luminosity function. Section 3 discusses the star formation rate at $z \simeq 0.2$. Our conclusions are presented in § 4.

2. THE Hα LUMINOSITY FUNCTION

The CFRS spectroscopic sample at $z \leq 0.3$ (138 galaxies) is a fair representation of field galaxies with absolute magnitudes in the range $-22 < M_{B_{AB}} < -14$ mag[2] and with $\langle z \rangle = 0.2086$ (see Fig. 1; also see § 2 in CFRS-XII for a detailed description). Because of the I-band ($\lambda_c = 8320$ Å) selection, these galaxies have been selected by light from the old stellar population rather than from their young stars. Consequently, our sample is less sensitive to galaxies undergoing strong recent star formation than B- or Hα-selected surveys at low z. The wide I band of width 2000 Å does not favor galaxies with strong Hα emission lines.

2.1. *The Emission-Line Measurements*

The spectral resolution is 40 Å; 117 out of the 138 spectra to $z = 0.3$ exhibit the blended emission line Hα + [N II] λλ6548, 65683 (hereafter Hα + [N II]). We have measured the integrated fluxes, equivalent widths, and the corresponding 1 σ errors for 110 blends (Hα + [N II]) with the package SPLOT under IRAF/CL. For seven spectra, the blended line could not be properly measured, since it was at the edge of the observed spectral window; in our statistical analysis, we considered them as not observed. The 1 σ errors in line flux are typically 10%, and the detection level ranges from 2.5 to 100 σ. Thus, these errors are not a significant source of uncertainty in our final estimate of the Hα luminosity function. Rest-frame equivalent widths (REW) are within the range 5–385 Å, and the mean is 48 Å. Only 6% of the Hα emitters have REW(Hα + [N II]) > 100 Å. In Figure 2, we show that except for three Hα emitters, the sample has a detection limit of REW at about 10 Å, and REW measurements are almost all above 3 σ. At $z \gtrsim 0.2$, the line [O II] can be detected. REW([O II]) are in the range 4–94 Å, with a mean of 14 Å. The CFRS spectra at $z \leq 0.3$ are limited in REW by the poor spectral resolution, rather than the signal-to-noise ratio, of the continuum because they are the result of ∼7 hours' exposure time. The 21 spectra with no detection of (Hα + [N II]) do not always show Hα in absorption, but all of them have the characteristics of absorption-line spectra: a strong 4000 Å break, Ca H and K, Hβ in absorption, G band, MgI, and a very red continuum [$(V - I_{AB}) \geq 1$].

2.2. *The* Hα *Flux Measurements*

To obtain the flux in Hα, we corrected the flux f(Hα + [N II]) from the contribution of the doublet [N II], where [N II] λ6583/[N II] λ6548 ∼ 3. Using results from a spectral analysis of the Stromlo-APM survey within the same absolute magnitude range as our emission-line galaxies ($-21 < M_B < -14$), we determined values of $N_2 = 1.33$[N II] λ6583/Hα ranging from 0.15 to 0.55 according to the strength of REW(Hα + [N II]) (Tresse, Maddox, & Loveday 1998). This method is in agreement with the trend of the average parameters of [N II] λ6583/Hα, EW(Hα), and $V - R$ colors of the UCM emission-lines galaxies (Gallego et al. 1997, Tables 1 and 2). Figure 3*b* shows the values we have taken.

Where possible, we estimated the interstellar extinction at Hα using the Hα/Hβ Balmer decrement. However, it is difficult to correct for reddening for all spectra because the 40 Å

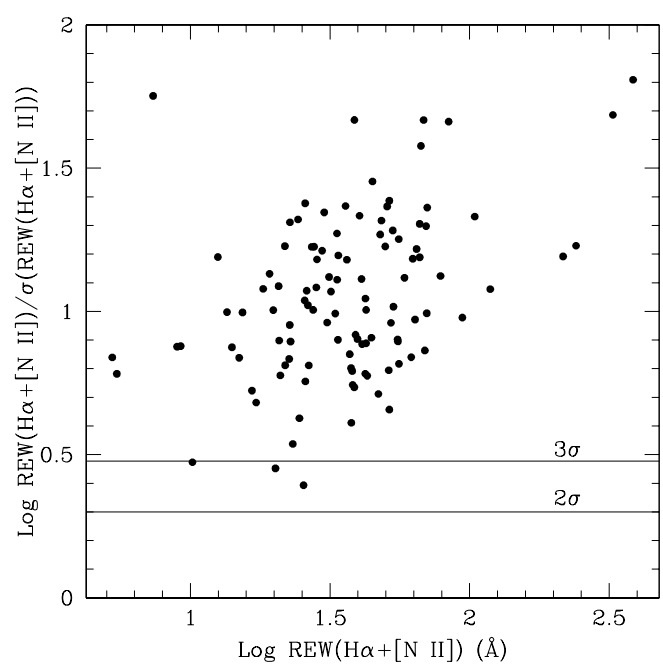

FIG. 2.—Detection level of REW(Hα + [N II]) vs. REW(Hα + [N II])

[2] We assumed $H_0 = 50$ km s^{-1} Mpc^{-1} and $q_0 = 0.5$ throughout the paper.

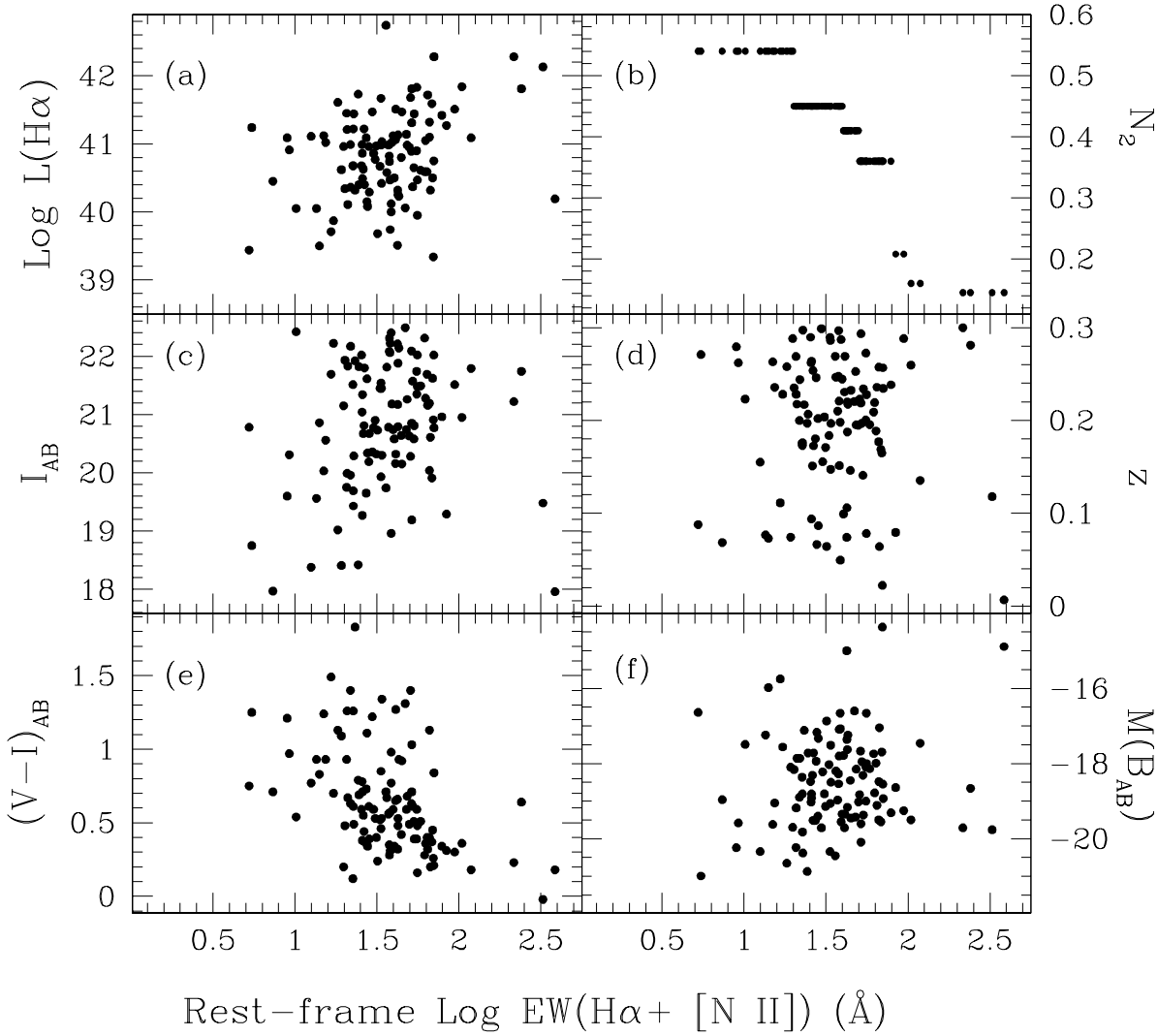

FIG. 3.—Relations between REW(Hα + [N II]) and other parameters as labeled. They are useful to compare our sample with other emission-line surveys.

spectral resolution and stellar absorption mean that Hβ is not always seen in emission. We were able to measure the Hβ integrated fluxes for 55 spectra. For those spectra where we could make a 3 σ measurement for Hβ (40 spectra), the extinction C has been measured in the following way:

$$10^{-C(-0.323)} = \frac{1}{2.86} \frac{f(\mathrm{H}\alpha + [\mathrm{N\ II}])/(1 + N_2)}{f(\mathrm{H}\beta)} . \quad (1)$$

The Hα/Hβ intensity ratio (2.86) is for case B recombination with a density of 100 cm^{-3} and a temperature of 10,000 K (Osterbrock 1989). $[X(\mathrm{H}\alpha) - X(\mathrm{H}\beta)]/X(\mathrm{H}\beta) = -0.323$ is the value given by the extinction law $X(\lambda)$ taken from Seaton (1979). We point out that although the different extinction laws are different in the UV, they behave similarly in the visible; hence, our results are independent of the choice made. For these 40 spectra, $\langle C \rangle = 0.36$. For the other 15 spectra with Hβ in emission, the average C is 0.82, or 0.50 if a 2 Å stellar absorption is accounted for at Hβ; we retained the latter value. For 10 spectra, we could not measure Hβ because of a sky line near it, and for the 44 remaining, Hβ is not detected in emission, probably because of stellar absorption. For these 54 spectra, we decided to apply a correction of $C = 0.45$, corresponding to a reddening parameter $A_V = CR/1.47 \simeq 1$ mag ($R = 3.2$; Seaton 1979), which is the average value measured by Kennicutt (1992) in nearby emission-line galaxies. We then corrected our Hα fluxes for reddening as follows:

$$\frac{f(\mathrm{H}\alpha + [\mathrm{N\ II}])}{1 + N_2} 10^{C(1-0.323)} . \quad (2)$$

We note that the final Hα luminosity densities using these reddening corrections are not significantly different from that using an average of $A_V = 1$ mag for all galaxies.

The 1″.75 spectral slits of the CFRS did not always contain the whole galaxy. To have consistent data, we corrected our fluxes by an aperture correction. For this, we integrated the spectral flux in the V band and transformed it into magnitudes. The spectrophotometric flux calibration across the spectra is generally accurate to better than 10% (see, e.g., Fig. 9 in Le Fèvre et al. 1995). The V magnitudes from the CFRS imaging are given by $I_{AB} + (V-I)_{AB}$, where I_{AB} is the isophotal magnitude and $(V-I)_{AB}$ is the color of the galaxy measured in an aperture of 3″. The aperture correction is $a = V_{\mathrm{image}} - V_{\mathrm{spectrum}}$. For our emission-line galaxies, the values range between 0 and 1.6 mag, with an average of 0.52. The dereddened Hα flux is then aperture

corrected to give the final estimate of the Hα fluxes:

$$f(\mathrm{H}\alpha) = \frac{f(\mathrm{H}\alpha + [\mathrm{N\ II}])}{1 + N_2}\, 10^{C(1-0.323)} 10^{0.4a} . \qquad (3)$$

Since at $z \simeq 0.26$ Hα falls at the center of our I band (8320 Å), we could check these aperture corrections, as follows. The integrated flux in ergs s^{-1} cm^{-2} in the blended line (Hα + [N II]) can also be computed using the observed EW(Hα + [N II]) in Å and the I-band magnitude in ergs s^{-1} cm^{-2} $\mathrm{Å}^{-1}$ to estimate the continuum flux such as

$$f(\mathrm{H}\alpha + [\mathrm{N\ II}]) = \mathrm{EW}(\mathrm{H}\alpha + [\mathrm{N\ II}])(1.5 \times 10^{-9}) 10^{-0.4 I_{AB}} . \qquad (4)$$

The differences between the two methods are small, of order 13%. They are due to the facts that the color $(V-I)_{AB}$ should be the one measured in the spectral slit, and not in a 3″ aperture, and that the true continuum level at Hα may not be exactly the mean value given by the I-band magnitude. These discrepancies are much smaller than our Poisson errors, so they do not affect our results on the Hα luminosity function. Another point is that according Kennicutt & Kent (1983), the Hα nuclear emission (H II region complexes in the inner disk and bulge regions) is, in general, rarely significant in comparison with the Hα emission from the whole galaxy. Hence, our aperture corrections should not overestimate the Hα measurements, even in the cases of starburst nuclei.

Finally, the Hα luminosity in ergs s^{-1} is given by

$$L(\mathrm{H}\alpha) = 4\pi (3.086 \times 10^{24} d_L)^2 f(\mathrm{H}\alpha) , \qquad (5)$$

where $f(\mathrm{H}\alpha)$ is the integrated flux in ergs s^{-1} cm^{-2} and d_L is the luminosity distance in Mpc.

2.3. *Calculation of the* Hα *Luminosity Function*

Figure 4 shows the comoving Hα luminosity density estimated from our raw data and from the data after applying each of the corrections described in § 2. These densities were

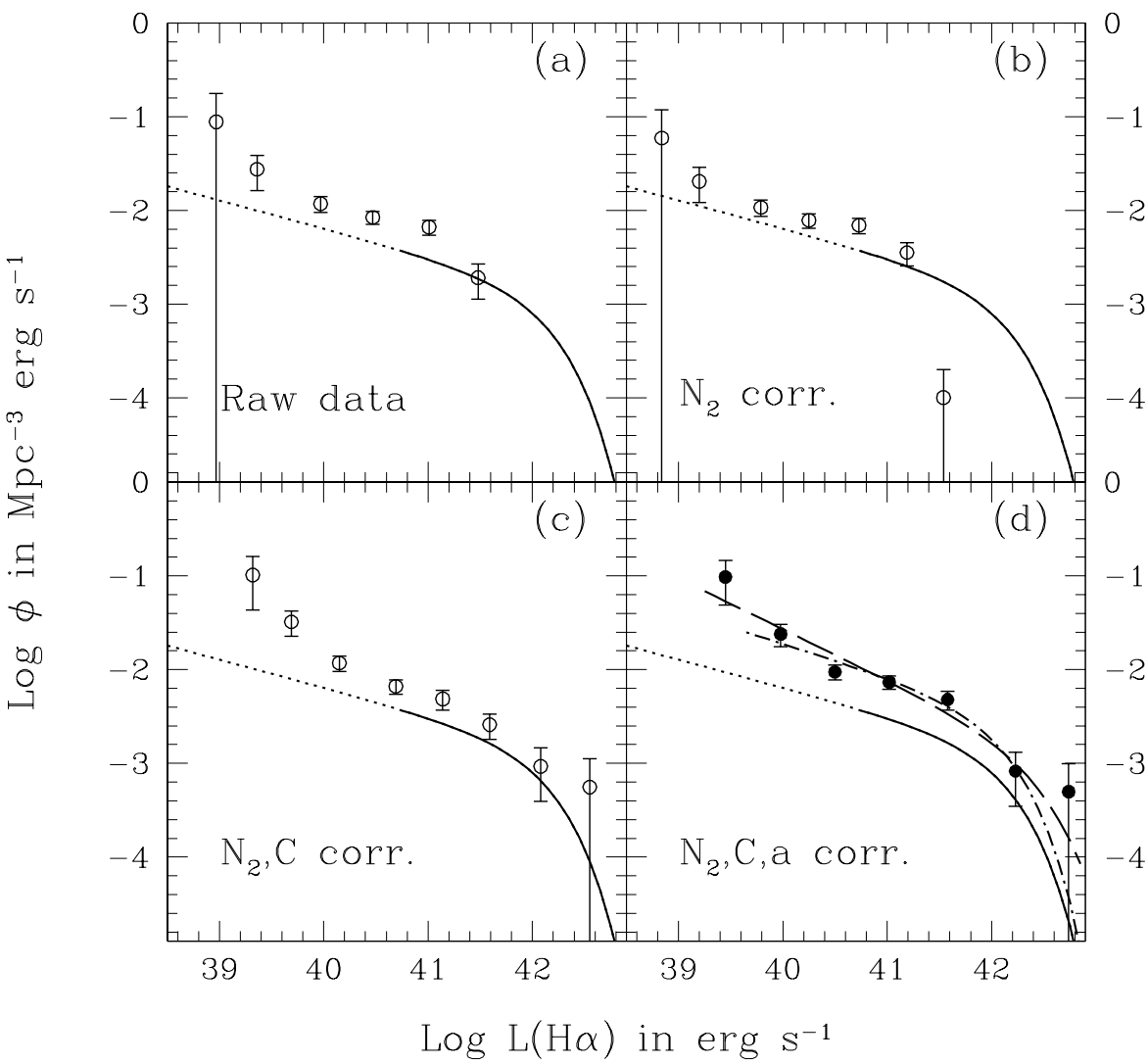

FIG. 4.—Overall Hα luminosity function at $z \leq 0.3$. The LFs with open circles show the successive corrections to obtain the final LF shown by the filled circles in panel (*d*). The raw data are shown in panel (*a*). Panel (*b*) shows this after correcting for the [N II] contribution to Hα (N_2). Panel (*c*) is further corrected for the reddening *C*. Applying the aperture correction *a* gives the final LF in panel (*d*). In each plot, the solid curve is the Gallego et al. (1997) Hα LF at $z \simeq 0$; the dotted curve is its extension to fainter luminosities. The long-dashed curves and dot-dashed curves are the best Schechter (1976) fits to our data; the latter one is given by excluding the faintest bin.

obtained using the $V_{\max}$ formalism, i.e.,

$$\phi[\log L(\mathrm{H}\alpha)]\Delta \log L(\mathrm{H}\alpha) = \sum_i \frac{1}{V^i_{\max}} . \quad (6)$$

$V^i_{\max}$ is the comoving volume in which galaxy i can be detected in this I-selected survey ($17.5 < I_{AB} < 22.5$), and the sum is over galaxies with Hα luminosity within the interval [$\log L(\mathrm{H}\alpha) \pm 0.5\Delta \log L(\mathrm{H}\alpha)$]:

$$V_{\max} = \int_{\max(z=0, I_{AB}=17.5)}^{\min(z=0.3, I_{AB}=22.5)} d^2_< \frac{dr}{dz} \Omega \, dz , \quad (7)$$

where $d^2_<$ is the angular distance, dr is the comoving distance at z, and Ω is the effective solid angle of the CFRS observations; five fields of $10'^2$ individually weighted by the number of spectroscopic observations out of the photometric observations. We plotted the comoving densities at the barycenter of the log $L(\mathrm{H}\alpha)$ of the N_i data belonging to the interval [$\log L(\mathrm{H}\alpha) \pm 0.5\Delta \log L(\mathrm{H}\alpha)$]. The density error bars are Poisson errors; $\log [1 \pm 1/(N_i)^{1/2}]$. Figure 4 shows also the Schechter (1976) fit to the local Hα luminosity function (LF) measured by Gallego et al. (1995) ($\alpha = -1.3$, $\phi^* = 10^{-3.2}$ Mpc^{-3}, $L^* = 10^{42.15}$ ergs s^{-1}).

Note that we used the $V_{\max}$ based on the I_{AB} magnitudes, since the galaxy selection is based on this measurement. For the lowest REW, our measurements are not absolutely complete, and so we should, in principle, include this effect in our estimates of $V_{\max}$. In practice, there is a strong correlation between $L(\mathrm{H}\alpha)$ and M_B (see Fig. 5*b*), which means that $V_{\max}$ should be only slightly smaller in these cases. We expect the difference in $V_{\max}$ to be small, since lines with low REW are observable even at our maximum redshift, $z = 0.3$, as can be seen in Figure 3*d*. An extreme upper limit to this effect can be obtained by artificially setting EW(Hα + [N II]) = 5 Å (roughly $+1\ \sigma$), or 1 Å for our non–Hα-emitting galaxies (15% of the sample). Then using the I_{AB} magnitudes, we can obtain an approximate flux in Hα + [N II], that we also corrected for N_2, C (taken as 0.45), and aperture as described in § 2.2. The LF we obtained in both cases is within the Poisson error bars of our actual results. As these 21 galaxies are very red, a small EW does not produce a small $L(\mathrm{H}\alpha)$, so they do not produce a steeper LF at the faint end. Thus, our estimated LF is quite stable.

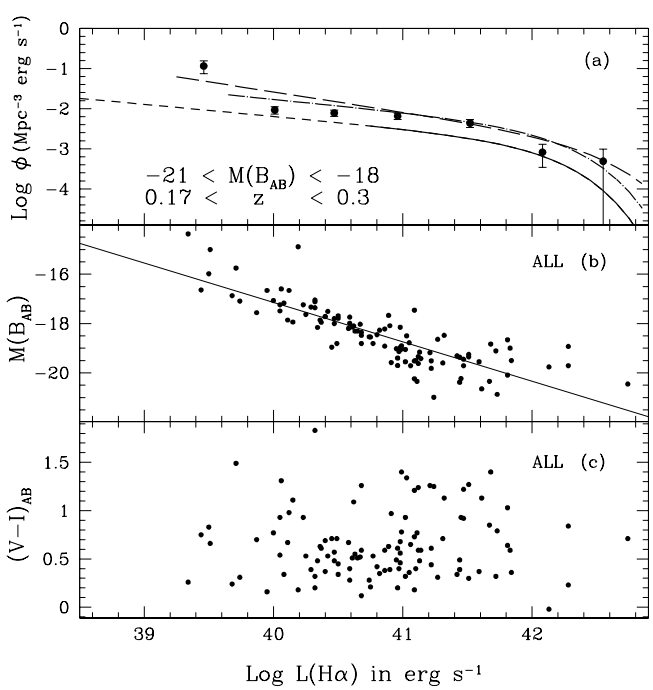

FIG. 5.—Panel (*a*) shows the Hα LF of the data within the rectangle shown in Fig. 1. The curves are the same as in Fig. 4*d*. Panels (*b*) and (*c*) show $M(B_{AB})$ and $(V-I)_{AB}$ vs. Hα luminosities of all the Hα emitters. Galaxies redder than a local Sb spiral have $(V-I)_{AB} \gtrsim 0.7$ at $z < 0.3$.

We fitted our overall Hα LF in Figure 4*d* with a Schechter function, and the best-fitting parameters given by a weighted minimum χ^2 are $\alpha = -1.54 \pm 0.08$, $\phi^* = 10^{-3.28 \pm 0.15}$ Mpc^{-3}, $L^* = 10^{42.50 \pm 0.23}$ ergs s^{-1}. If we exclude the faintest bin from the fit which contains only four galaxies, we find

$$\alpha = -1.35 \pm 0.06 ,$$
$$\phi^* = 10^{-2.83 \pm 0.09} \ \mathrm{Mpc}^{-3} ,$$
$$L^* = 10^{42.13 \pm 0.13} \ \mathrm{ergs\ s}^{-1} .$$

The quoted errors are the formal χ^2 fit standard deviations, assuming the parameters are uncorrelated. In fact, these three parameters are highly correlated, so the formal errors are not realistic estimates; the difference between these two fits give a realistic estimate of the true errors. Figure 1 shows that at different redshifts, our survey does not sample exactly the same range of absolute magnitudes. In principle, this could affect our LF, so we calculated the Hα LF using only the galaxies at $0.17 < z < 0.3$ and $-18 < M(B_{AB}) < -21$, i.e. where the data constitute an homogeneous subsample. The result is shown in Figure 5*a*, and we can see that the resulting densities are entirely consistent with our fitted LFs.

Our Hα LF at $z \leq 0.3$ samples fainter Hα luminosities than the Gallego et al. (1995) LF; their lowest data is above log $L(\mathrm{H}\alpha) = 40.4$ ergs s^{-1}, ours is at 39.2 ergs s^{-1}. On the other hand, the ($I_{AB} < 17.5$) CFRS limit and ($z < 0.3$) cut lead to a small volume where we sample bright galaxies with $M_{B_{AB}} < -21$ mag. According to Figure 5*b*, this corresponds to log $L(\mathrm{H}\alpha) \gtrsim 42.3$ ergs s^{-1}, which explains the large statistical error on our brightest Hα luminosity bin. Also, our sample contains a larger proportion of emission-line galaxies with 5 < REW(Hα + [N II]) < 30 Å. This can be seen in comparing Figures 9 and 10 in Gallego et al. (1997) and our Figures 3*c* and 3*d*.

Although it may be expected that blue galaxies correspond to star-forming galaxies, Figure 5*c* shows that there is not a clear correlation between the $(V-I)$ color of a galaxy and $L(\mathrm{H}\alpha)$ in our sample. There is, however, a trend seen in Figure 5*e*, implying blue galaxies tend to have higher REW(Hα + [N II]). The latter is in agreement with Figure 10 in Kennicutt & Kent (1983), which plots REW(Hα + [N II]) against $B-V$ colors for a nearby sample of Sa-Irr galaxies. These figures show that REW(Hα) is sensitive to the ratio of ionizing stars (which produce Hα) to lower mass red giant stars (which produce the stellar continuum at Hα).

On the one hand, this means that we have detected red[3] galaxies that show both low and high Hα fluxes and that these contribute to the overall luminosity as well as the blue galaxies, for which emission lines are easier to detect

[3] At $z < 0.3$, galaxies having $V - I_{AB} \gtrsim 0.7$ are redder than a local Sb spiral (see Fig. 13 in Tresse et al. 1996).

because of a lower stellar continuum at Hα. Following the terminology in Gallego et al. (1997), these red galaxies are likely to correspond to starburst nuclei galaxies (SBN) if Hα is bright and to dwarf amorphous nuclear starbursts (DANS) when log L(Hα) < 41.6. Both classes are spiral galaxies. According to Tresse et al. (1996) and Gallego et al. (1997), they represent ∼40% of emission-line galaxies, the remaining being spectrally classified as H II galaxies, blue compact galaxies, or active galaxies.

On the other hand, the lack of a correlation between Hα luminosities and continuum colors means that Hα production is independent of the overall stellar content and depends only on the recent star formation. The observed $(V-I)_{AB}$ at $0.1 < z < 0.3$ is rest-frame $(B-R)_{AB}$, which may be significantly reddened. However, the typical reddening is $(A_B - A_R) \sim 0.2$ mag, which would not make blue galaxies appear as red as we observe. The independence of L(Hα) on total stellar content can also be seen in the fact that red galaxies classified in class (B) by Tresse et al. (1996) often show spectral features proving the presence of a dominant old stellar population (Ca H and K, G band, MgI; see Fig. 1 of Tresse et al. 1996). So, we suspect that some red galaxies show recent star formation similar to blue galaxies.

Figure 5*b* shows a tight relation between Hα luminosities and B luminosities, both of which are closely related to recent star formation. A least-squares fit gives

$$M(B_{AB}) = 46.7 - 1.6 \log L(\mathrm{H}\alpha) . \quad (8)$$

If this relation holds at higher redshifts, $0.3 < z < 1$, we would expect that the high-z CFRS galaxies, which are brighter than −20 in B, should exhibit stronger Hα emission lines than those observed locally. This is in agreement with the results of Hammer et al. (1997), who found a large increase in the comoving [O II] luminosities up to $z \sim 1$ in the CFRS ([O II] luminosities being indirectly related to Hα luminosities).

3. STAR FORMATION RATE AT $z \simeq 0.2$

We integrated our best-fit luminosity function to give the overall comoving luminosity density at $\langle z \rangle = 0.2$:

$$\mathscr{L}(\mathrm{H}\alpha) = \int_0^\infty \phi(L) L \, dL = \phi^* L^* \Gamma(2+\alpha) . \quad (9)$$

We then find a total Hα luminosity per unit volume ranging from $10^{39.44 \pm 0.04}$ to $10^{39.50 \pm 0.07}$ ergs s^{-1} Mpc^{-3} at $z \simeq 0.2$ from our two previous LF best fits. The errors quoted here are the standard deviations taking into account that the three Schechter parameters are correlated, and so should be realistic estimates. Our value is 2.2–2.6 times higher than the value of Gallego et al. (1995) at $z \sim 0$ ($10^{39.09 \pm 0.04}$, see the erratum to Gallego et al. 1995). Consequently, our result shows that the star formation rate (SFR) is higher at $z \simeq 0.2$ than that found in the local universe for galaxies with REW(Hα + [N II]) $\gtrsim$ 10 Å. Figure 6 shows our data and the local measurements in the SFR versus z plot from Madau, Pozzetti, & Dickinson (1998) assuming a Salpeter (1955) initial mass function (IMF) including stars in the mass range $0.1 < M < 125\ M_\odot$. We used their conversion $\mathscr{L}(\mathrm{H}\alpha) = 10^{41.15}$ SFR/($M_\odot$ yr^{-1}), based on the stellar population synthesis models of Bruzual & Charlot (1997). The other points in this plot are from rest-frame UV continuum measurements. The comparison between the UV and Hα results is not straightforward for the following reasons. As

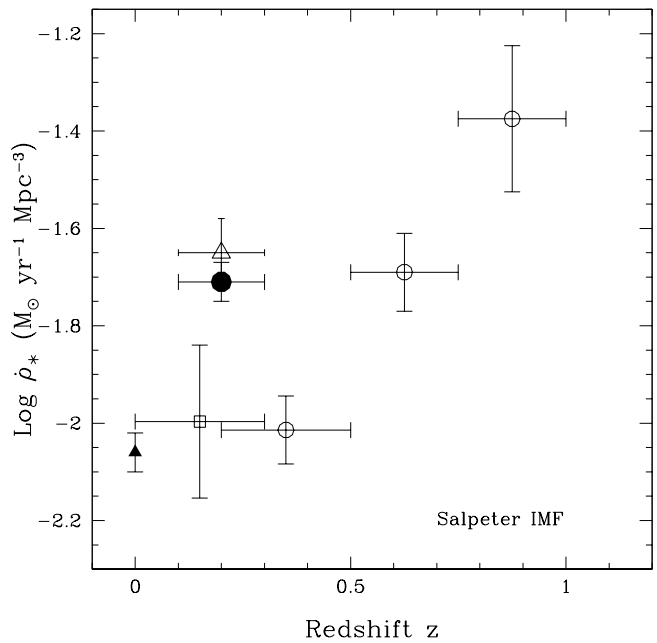

FIG. 6.—Comoving volume-averaged star formation rate vs. redshift. The open circles are from the "LF-estimated" UV(2800 Å) CFRS data of Lilly et al. (1996), the open square is from UV(2000 Å) data of Treyer et al. (1997), and the filled triangle is from Hα data of Gallego et al. (1995). The filled circle is our Hα result (the open star is our result if the faintest bin of our Hα LF is included). We used the Madau et al. (1998) conversion factors, log $\mathscr{L}(\mathrm{H}\alpha) = 41.15 + \log \dot{\rho}_*$, and log $\mathscr{L}_{\mathrm{UV}} = 27.9 + \log \dot{\rho}_*$, assuming a Salpeter IMF and including stars in the 0.1–125 $M_\odot$ mass range.

noted in the introduction, Hα fluxes come from ionized gas surrounding OB stars, and so are directly correlated to short-lived stars, once they are dust corrected with the Balmer decrement. The UV continuum comes from both short- and long-lived stars; the long-lived (late B, A0) stars contribute more to the UV continuum at larger UV wavelengths. In addition, Calzetti (1997) pointed that longer-lived nonionizing stars are likely to be found in less obscured regions, than ionizing stars. This agrees with observations of starbursts where the extinction obtained with the Balmer decrement is found to be higher than the extinction obtained from UV continuum (Keel 1993). Given that UV photons are more obscured than Hα photons, we expect that UV data should be less correlated to short-lived stars than Hα data. Overall, converting Hα luminosities to SFR depends less sensitively on the dust correction than on the assumed IMF. Converting UV luminosities to SFR depends less sensitively on IMFs in a standard cosmology (Baugh et al. 1997) than on uncertain dust extinction.

In Figure 6, the Hα data are reddening corrected, while UV data are not; thus, Hα data must give higher values of star formation rate than their counterpart in the UV. Calzetti et al. (1994) measured an *effective* dust extinction law from a sample of extended regions such as the central regions of starburst and blue compact galaxies. Their law is characterized by the absence of a 2175 Å dust feature. Assuming $A_V = 1$ mag, it predicts an average dust extinction at 2000 Å that is 1.95 times more in flux than at Hα. Treyer et al. (1997) have a preliminary measurement of the UV(2000 Å) density at $z = 0.15$ and find it is consistent with the UV(2800 Å) CFRS data (Lilly et al. 1996). According to the results from Calzetti (1997), our Balmer decrement

reddening of $A_V = 1$ mag would imply that the UV stellar continuum at 2000 and 2800 Å has an extinction of 1.3 and 1 mag, respectively. Thus, our SFR result at $\langle z \rangle = 0.2$ seems to be consistent with the UV(2000 Å) data at $\langle z \rangle = 0.15$ and the UV(2800 Å) data at $\langle z \rangle = 0.35$ within the error bars.

4. CONCLUSION

We constructed an optically selected Hα luminosity function at $z \simeq 0.2$; this will be useful as a comparison to future near-infrared spectroscopic surveys that will detect Hα in galaxies near the expected peak of SFR. We find a total Hα luminosity at least twice that of the one measured in the local universe by Gallego et al. (1995) for galaxies with REW(Hα + [N II]) $\gtrsim$ 10 Å. If the SFR evolution follows a $(1 + z)^3$ law, then $\mathscr{L}$(Hα) should decrease by a factor of 1.7 from $z = 0.2$ to $z = 0$. This factor is marginally outside the 1 σ errors and may suggest that the local Hα density is low by $\sim$20%. This may correspond to the local underdensity seen in optical redshift surveys (see Zucca et al. 1997). If the local estimate is correct, then it implies an evolution proportional to $(1 + z)^{4.4}$. Another possibility that could explain this 20% discrepancy is that we did not exclude AGN galaxies, which may represent 8%–17% of our sample (Tresse et al. 1996), whereas Gallego et al. (1995) did exclude AGN galaxies.

Since the number of hydrogen-ionizing photons ($\lambda < 912$ Å) emitted by a star is proportional to the Hα recombination line, the total flux in Hα is a good tracer of the number of ionizing stars within emission-line galaxies. The IMF introduces uncertainties in the relation between Hα luminosity and star formation rate; Hα traces only the massive, hot, short-lived stars, and therefore assumptions on the remaining fraction of cooler stars have to be made. Also, since star formation takes place in highly obscured regions, newly formed stars are not detected in the UV or optical observations. Taking the SFR factor conversions from Madau et al. (1998), our result is consistent with UV data corrected for $\sim$1 mag of dust extinction. Larger dust corrections would imply either an IMF with a shallower slope than the one from Salpeter or an underestimation of the total Hα luminosity. However, we are aware that uncertainties in models and in UV dust extinction are still large.

Another interesting result is the strong correlation observed between the flux emitted in the rest-frame B band and Hα luminosity. Applying this relation to the CFRS where the rest-frame B band is directly observed at $z = 0.9$, the range of sampled magnitudes suggests that all emission-line galaxies should be strong Hα emitters. This is in agreement with Hammer et al. (1997), who find an increase of the comoving number of [O II] CFRS emitters by a factor at least 5 up to $z \sim 1$. This correlates with the evolution seen in the CFRS LFs, which is due to these bright, star-forming galaxies. At high redshifts, deep spectroscopic surveys clearly become biased toward strong emission-line, dust-free emitters, which contribute to the increase of the total luminosity of these galaxies at earlier epochs; however, they may be only the tip of the iceberg of all Hα emitters.

It is a pleasure for L. T. to thank her colleagues David Crampton, François Hammer, Olivier Le Fèvre, and Simon Lilly, who made the CFRS survey possible. This work has benefited from fruitful discussions with Stephane Charlot. We thank Piero Madau, who kindly provided his most recent SFR conversion factors. L. T. acknowledges support from the European Commission HCM program contract ERB CHBICT941612. S. J. M. acknowledges support from a PPARC advanced fellowship.

REFERENCES

Baugh, C. M., Cole, S., Frenk, C. S., & Lacey, C. G. 1997, ApJ, in press
Bruzual, G., & Charlot, S. 1997, in preparation
Calzetti, D. 1997, in Proceedings of the conference "The Ultraviolet Universe at Low and High Redshift," College Park, MD, 1997 May 2–4, ed. W. Waller, M. N. Fanelli, J. E. Hollis, & A. C. Danks (New York: AIP), in press (astro-ph/9706121)
Calzetti, D., Kinney, A. L., & Storchi-Bergmann, T. 1994, ApJ, 429, 582
Crampton, D., Le Fèvre, O., Lilly, S. J., & Hammer, F. 1995, ApJ, 455, 96
Ellis, R. S., Colless, M., Broadhurst, T. J., Heyl, J., & Glazebrook, K. 1996, MNRAS, 280, 235
Gallego, J., Zamorano, J., Aragón-Salamanca, A., & Rego, M. 1995, ApJ, 455, L1; erratum, 459, L43 (1996)
Gallego, J., Zamorano, J., Rego, M., & Vitores, A. G. 1997, ApJ, 475, 502
Hammer, F., Flores, H., Lilly, S. J., Crampton, D., Le Fèvre, O., Rola, C., Mallen-Ornelas, G., Schade, D., & Tresse, L. 1997, ApJ, 481, 49
Keel, W. C. 1993, in ASP Conf. Ser. 35, Massive Stars: Their Lives in the Interstellar Medium, ed. J. P. Cassinelli & E. B. Churchwell (San Francisco: ASP), 498
Kennicutt, R. C. 1992, ApJ, 388, 310
Kennicutt, R. C., & Kent, S. M. 1983, ApJ, 88, 1094
Le Fèvre, O., Crampton, D., Lilly, S. J., Hammer, F., & Tresse, L. 1995, ApJ, 455, 60
Lilly, S. J., Le Fèvre, O., Crampton, D., Hammer, F., & Tresse, L. 1995a, ApJ, 455, 50
Lilly, S. J., Le Fèvre, O., Hammer, F., & Crampton, D. 1996, ApJ, 460, L1
Lilly, S. J., Tresse, L., Hammer, F., Crampton, D., & Le Fèvre, O. 1995c, ApJ, 455, 108
Madau, P., Ferguson, H. C., Dickinson, M. E., Giavalisco, M., Steidel, C. C., & Fruchter, A. 1996, MNRAS, 283, 1388
Madau, P., Pozzetti, L., & Dickinson, M. E. 1998, ApJ, in press
Osterbrock, D. E. 1989, Astrophysics of Gaseous Nebulae and Active Galactic Nuclei (Mill Valley: University Science Books)
Salpeter, E. E. 1955, ApJ, 121, 61
Sarajedini, V. L., Green, R. F., Griffiths, R. E., & Ratnatunga, K. 1996, ApJ, 471, L15
Schechter, P. 1976, ApJ, 203, 297
Seaton, M. J. 1979, MNRAS, 187, 73
Steidel, C. C., Giavalisco, M., Pettini, M., Dickinson, M., & Adelberger, K. L. 1996a, ApJ, 462, L17
Tresse, L., Maddox, S. J., & Loveday, J. 1998, MNRAS, in preparation
Tresse, L., Rola, C., Hammer, F., Stasińska, G., Le Fèvre, O., Lilly, S. J., & Crampton, D. 1996, MNRAS, 281, 847 (CFRS-XII)
Treyer, M. A., Ellis, R. S., Milliard, B., & Donas, J. 1997, in Proceedings of the conference "The Ultraviolet Universe at Low and High Redshift," College Park, MD, 1997 May 2–4, ed. W. Waller, M. N. Fanelli, J. E. Hollis, & A. C. Danks (New York: AIP), in press
Zucca, E., et al. 1997, A&A, 326, 477